WWW.IJRPR.COM

International Journal of Research Publication and Reviews

Journal homepage: www.ijrpr.com ISSN 2582-7421

Advanced MATLAB Simulation of Electric Vehicle DC-DC Buck Converter with Brushless DC Motor Integration

Mr. Sanjay Bisen[1], Abhishek Agwekar[2]

[1]M. Tech Scholar, Truba Collage of science and technology, Bhopal M.P.
[2]Asso. Prof. and HOD EX Truba Collage of science and technology, Bhopal M.P.

Abstract

This study presents an advanced MATLAB simulation framework for an electric vehicle (EV) system integrating a DC-DC buck converter and a Brushless DC (BLDC) motor. The primary objective is to enhance energy efficiency, motor control precision, and overall system performance in EV applications. The buck converter is modeled to regulate voltage efficiently, ensuring optimal power delivery to the BLDC motor under varying load and operational conditions. A dynamic model of the BLDC motor is incorporated, capturing its electrical and mechanical characteristics to analyze speed, torque, and efficiency profiles. Furthermore, the simulation includes a feedback-based control strategy for achieving stable and precise operation of the motor, even during rapid load changes or voltage fluctuations. This work highlights the importance of power electronics in modern EV systems and provides a robust platform for testing and optimizing EV power train components. The proposed model can serve as a foundation for further research in advanced EV control strategies and energy management systems.

Keywords: Electric Vehicle, charging station, optimal location, voltage impact, combustion engine vehicles, gas-powered vehicles, Provincial Electricity Authority.

1.1 Introduction

Global warming remains one of the most pressing challenges worldwide, primarily driven by carbon emissions from combustion engine vehicles, which significantly contribute to climate change and natural disasters. In response to these concerns, Smart Grids (SG) are emerging as a cleaner energy solution compared to traditional grids. Coupled with electric vehicles (EVs), which are far more eco-friendly than conventional gasoline-powered vehicles, the integration of smart grids and EVs has the potential to yield substantial environmental benefits.

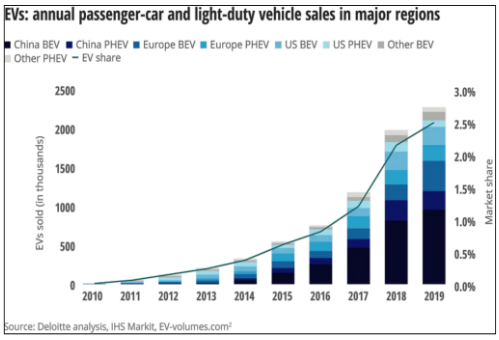

Figure 1 :-annual Passenger car and light duty vehicle sales

Recognizing this opportunity, the Provincial Electricity Authority (PEA) has unveiled its visionary SG Roadmap project. This initiative focuses on leveraging advanced technologies to optimize the generation and distribution of renewable energy, thereby reducing reliance on fossil fuels. As part of this project, a robust EV charging infrastructure will be developed across Thailand, laying the foundation for a sustainable and energy-efficient future.

1.2 Problem Statement

The author aims to explore methods for identifying optimal locations for EV charging stations by analyzing the real-world behavior of EV users and assessing the impact of charging on power distribution systems. This study proposes leveraging Geographical Information Systems (GIS) data provided

by the Provincial Electricity Authority (PEA) to develop an adaptive and practical approach. The goal is to establish a model for EV charging infrastructure that effectively integrates charging stations into real-world transportation systems to meet the needs of EV users.

1.3 Motivation for Vehicle Electrification

Over the past few decades, the growing emphasis on environmental sustainability and the finite nature of petroleum-based resources have driven a shift in the automotive industry toward sustainable transportation solutions. Electrification of vehicles has emerged as a key approach, replacing traditional mechanical systems with electric-powered architectures to reduce emissions and enhance performance. The push for electrified vehicles stems from several compelling factors:

1. Higher Energy Efficiency,
2. Enhanced Fuel Economy
3. Better Acceleration:

1.4 Background of Electrical Vehicle

The placement of EV charging stations must consider the impact on power distribution systems. The sudden surge in demand for electricity at specific locations can strain the grid, leading to voltage fluctuations, increased losses, and potential power quality issues. Therefore, it is imperative to install charging stations in a way that minimizes disruptions to the existing power infrastructure. This requires a detailed understanding of power flow dynamics, load distribution, and the potential impact of EV charging behavior on the electrical grid.

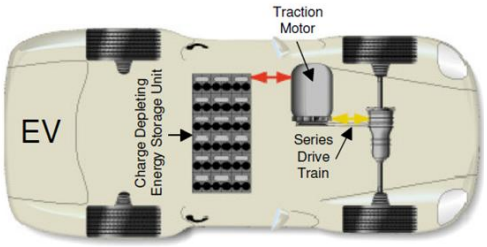

Figure 2:- Electrical Vehicle for traction Motor Drive

This study introduces a novel approach to addressing these challenges by proposing a systematic method for determining optimal locations for EV charging stations. The methodology leverages real-time data on road traffic volume and vehicle driving ranges, collected through mobile logs. This data-driven approach provides valuable insights into the movement patterns of EV users, allowing planners to identify areas with high demand for charging services. By analyzing potential electricity depletion points, the proposed algorithm pinpoints the best locations for installing charging stations, ensuring maximum convenience for users and optimal utilization of resources. The development of high-energy magnetic materials and the introduction of advanced power electronics—such as thyristors and power MOSFETs—breathed new life into the technology. By the 1980s, these innovations allowed for the creation of more powerful and efficient BLDC motors, and the first models using thyristors were designed. In the late 1980s, Robert E. Lordo, working with POWERTEC Industrial Corporation, successfully designed the first large-scale brushless DC motors with power ratings of 50 horsepower and above. These breakthroughs paved the way for the widespread use of BLDC motors in various industrial applications, showcasing their versatility and performance capabilities. Overall BLDC Motor Drive Block diagram shown in fig.3.1.

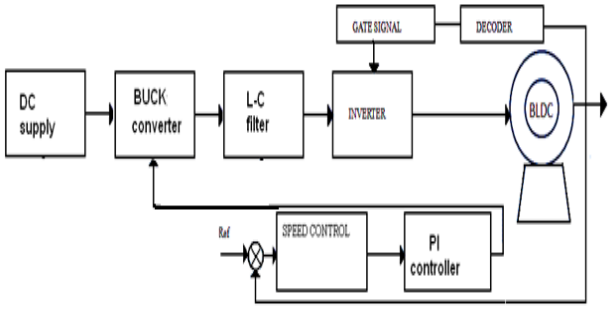

Fig3:- Overall Block Diagram of the BLDC Motor Drive

Today, virtually all leading motor manufacturers produce brushless DC motors. These motors have made a significant impact in various industrial sectors, particularly in applications such as plastics and fiber production, wire drawing, winding systems, cranes, and conveyors. More recently, a mining company has adopted several 300-horsepower brushless DC motors to power coal conveyors in underground mines.

1.5 DETAILS OF STATE SPACE MODELING

The coupled circuit equations of the stator windings in terms of motor electrical constants are

$$\begin{bmatrix} V_{as}-v_n \\ V_{bs}-v_n \\ V_{cs}-v_n \end{bmatrix} = \begin{bmatrix} R_s & 0 & 0 \\ 0 & R_s & 0 \\ 0 & 0 & R_s \end{bmatrix} \begin{bmatrix} I_a \\ I_b \\ I_c \end{bmatrix} + p \begin{bmatrix} L_{aa} & L_{ab} & L_{ac} \\ L_{ba} & L_{bb} & L_{bc} \\ L_{ca} & L_{cb} & L_{cc} \end{bmatrix} \begin{bmatrix} I_a \\ I_b \\ I_c \end{bmatrix} + \begin{bmatrix} E_a \\ E_b \\ E_c \end{bmatrix} \quad \text{-----eq (1)}$$

Where:
R: Stator resistance per phase
$I_a I_b$, *Ic*: Stator phase currents
p: *d/dt* is the time derivative operator
E_a, E_b, E_c : represent the back emfs in the respective phases in (1)
v_n : is the neutral point node voltage given by

$$v_n = \frac{1}{3}\left[V_{as} + V_{bs} + V_{cs}\right] - \sum BEMFs \quad \text{----eq (2)}$$

$\sum$ *BEMFs* means summing up the individual phase emfs on an instant to instant basis.
The induced emfs are all assumed to be trapezoidal, whose peak value is given by:
Ep= (BLv) N = N (Blr ω) = NΦ ω= λ ω. ------eq (3)
Where:
B is the flux density of the field in Weber's
L is the rotor length
N is the number of turns per phase
ω is the electrical angular speed in rad/sec
Φ represents flux linkage=BLr
λ represents the total flux linkage given as the product number of conductors and flux linkage/conductor.
If there is no change in rotor reluctance with angle because of no salient rotor and assuming three symmetric phases, inductances and mutual inductances are assumed to be symmetric for all phases, i.e. (1) becomes:

$$\begin{bmatrix} V_a \\ V_b \\ V_c \end{bmatrix} = R_s * \begin{bmatrix} 1 & 0 & 0 \\ 0 & 1 & 0 \\ 0 & 0 & 1 \end{bmatrix} \begin{bmatrix} I_a \\ I_b \\ I_c \end{bmatrix} + p \begin{bmatrix} L & M & M \\ M & L & M \\ M & M & L \end{bmatrix} \begin{bmatrix} I_a \\ I_b \\ I_c \end{bmatrix} + \begin{bmatrix} E_a \\ E_b \\ E_c \end{bmatrix} \quad \text{-----eq (4)}$$

Simplifying (3) further we get equation (4)

$$\begin{bmatrix} Vas \\ Vbs \\ Vcs \end{bmatrix} = R_s * \begin{bmatrix} 1 & 0 & 0 \\ 0 & 1 & 0 \\ 0 & 0 & 1 \end{bmatrix} \begin{bmatrix} I_a \\ I_b \\ I_c \end{bmatrix} + p \begin{bmatrix} L-M & 0 & 0 \\ 0 & L-M & 0 \\ 0 & 0 & L-M \end{bmatrix} \begin{bmatrix} I_a \\ I_b \\ I_c \end{bmatrix} + \begin{bmatrix} E_a \\ E_b \\ E_c \end{bmatrix} \quad \text{--eq(5)}$$

The generated electromagnetic torque is given by

$$T_e = [E_a I_a + E_b I_b + E_c I_c]/\omega \text{ (in N.m)} \quad \text{--eq (6)}$$

The induced emfs can be written as

$$E_a = fa(\theta)\lambda\ \omega.$$
$$E_b = fb(\theta)\lambda\ \omega. \quad \text{----------eq (7)}$$
$$E_c = fc(\theta)\lambda\ \omega.$$

Where:

fa(θ), fb(θ) and fc(θ) are functions having same shapes as back emfs with maximum magnitude of ± 1.These are written as 'LA', 'LB','LC' in the file 'Brushless DC Motor'.

These values from (6) can be substituted in (5) to obtain the value of torque. Also,

$$J(d\omega/dt) + B\omega = T_e - T_l \quad \text{------eq(8)}$$

Where:
T_l : load torque
J: moment of inertia
B: friction coefficient.
Electrical rotor speed and position are related by
d θ/dt = (P/2)* ω --------eq (9)
Where P is the number of poles in the motor.

Combining all the equations, the system space form becomes

X' = Ax + Bu ----------eq(10)

$$\text{Where } x = \begin{bmatrix} I_a & I_b & I_c & \omega & \theta \end{bmatrix}^T$$ -----eq (11)

Thus the state space matrix becomes:

$$A = \begin{bmatrix} -R_S/L_1 & 0 & 0 & (\lambda p * f_a(\theta))/L_1 & 0 \\ 0 & -R_s/L_1 & 0 & (\lambda p * f_b(\theta))/L_1 & 0 \\ 0 & 0 & -R_s/L_1 & (\lambda p * f_s(\theta))/L_1 & 0 \\ (\lambda p * f_a(\theta))/J & (\lambda p * f_b(\theta))/J & (\lambda p * f_c(\theta))/J & -B/J & 0 \\ 0 & 0 & 0 & P/2 & 0 \end{bmatrix}$$ ---eq (12)

$$B = \begin{bmatrix} 1/L_1 & 0 & 0 & 0 \\ 0 & 1/L_1 & 0 & 0 \\ 0 & 0 & 1/L_1 & 0 \\ 0 & 0 & 0 & -1/J \\ 0 & 0 & 0 & 0 \end{bmatrix}$$ ------eq (13)

and

$$U = \begin{bmatrix} V_a & V_b & V_c & T_l \end{bmatrix}^T$$ -----eq (14)

Where:
L_1: L-M;
L: self inductance of the winding per phase
M: The mutual inductance per phase
V_a, *Vb*, *Vc*, are the per phase impressed voltages on the motor windings.
All the equations form the entire state space model for the BLDC.
Consistent system of units must be used.
The closed-loop system is modeled and simulated using MATLAB Simulink. The Simulink representation of the MATLAB buck converter is shown in Fig. 5.1. In this system, a 48V DC input is stepped down to 24V DC through a buck converter. The buck converter's output is then smoothed using a PI filter. This filtered DC voltage is supplied to a three-phase inverter, which generates the three-phase AC voltage required to drive the PMBLDC motor.

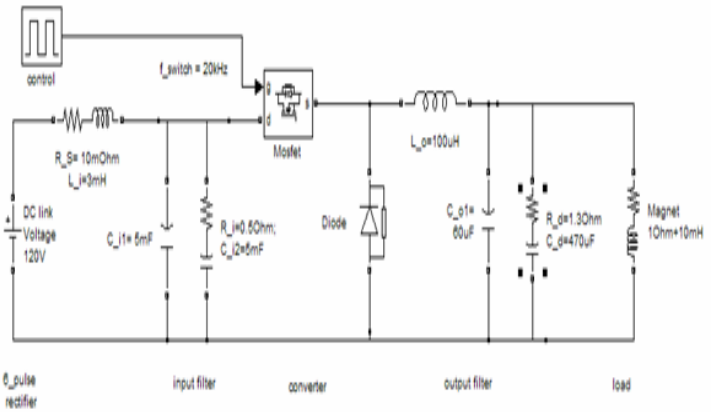

Fig. 4 :- MATLAB Simulink Model for Buck Converter

Converter data

The 3dB cutoff frequency of the input filter is set at 30 Hz, with Li=3 mHL_i = 3 \, \text{mH}Li=3mH and Ci1+Ci2=10 mFC_{i1} + C_{i2} = 10 \, \text{mF}Ci1+Ci2=10mF. While the ripple frequency of a 6-pulse rectifier is 300 Hz, a 50 Hz component is also anticipated in the DC-link voltage due to mains voltage asymmetry. The maximum current ripple through LoL_oLo is limited to 15% of the maximum DC current, equivalent to 15 App_{\text{pp}}pp. The 3dB cutoff frequency of the output filter is set one decade below the switching frequency, at 2 kHz, with Lo1=100 µHL_{o1} = 100 \, \mu \text{H}Lo1=100µH and Co1=60 µFC_{o1} = 60 \, \mu \text{F}Co1=60µF. Both input and output filters are damped with small resistors connected in series with their capacitors, and the filters are coupled through the FET.

The stator windings are connected in a star configuration to an internal neutral point. The motor's actual speed is measured and compared to the reference speed, with the resulting error fed into a PI controller. The PI controller's output serves as one input to a comparator, while the other input is a high-frequency triangular wave. The comparator's output determines the pulse width applied to the buck MOSFET. The gate pulses for MOSFETs 1, 3, and 5 are depicted in Fig. 5.7. The DC input voltage, shown in Fig. 5.6, is 48 volts. The phase voltages of the three-phase inverter, displaced by 120º,

are shown in Fig. 5.8, while the corresponding three-phase currents drawn by the motor are illustrated in Fig. 5.9. The back EMFs in the three phases are displayed in Fig. 5.10. Finally, the speed response is presented in Fig. 5.13, where the speed stabilizes at 130 rpm, matching the set value shown in Fig. 5.14.

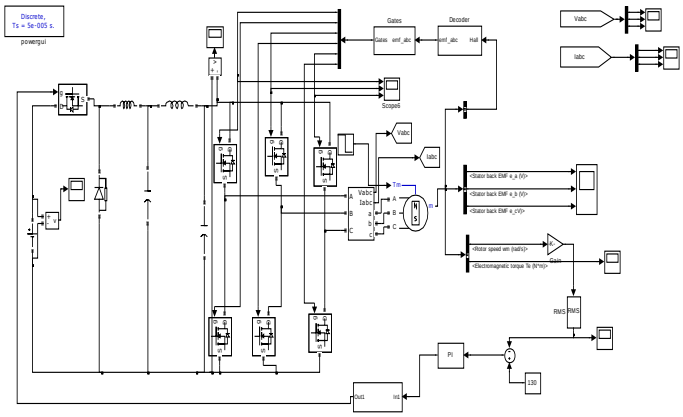

Fig.5:-The Simulink diagram of Buck Converter inverter fed PMBLDC drive.

RESULT:

The input DC voltage is determined to be 48 volts. A buck converter steps this down to 24 volts, which is then supplied to a three-phase inverter. The inverter transforms the DC voltage into AC, and this AC output powers a brushless DC (BLDC) motor.

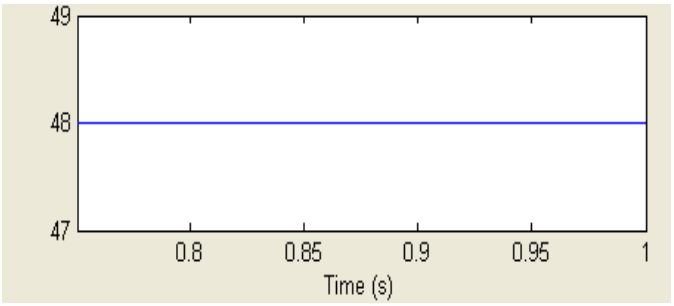

Fig:-6:-The input dc voltage.

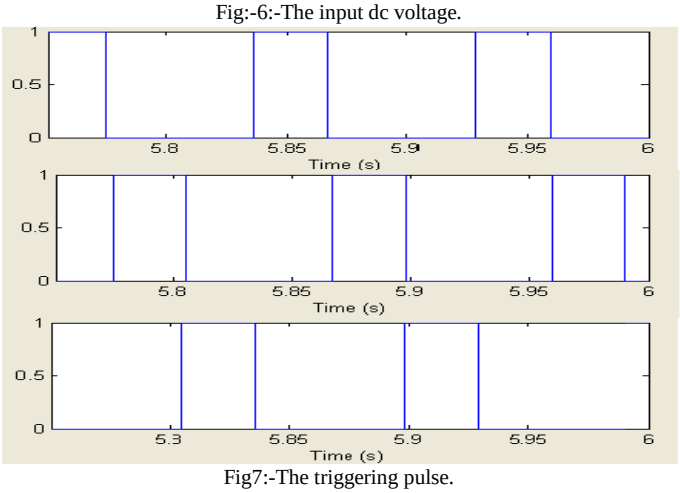

Fig7:-The triggering pulse.

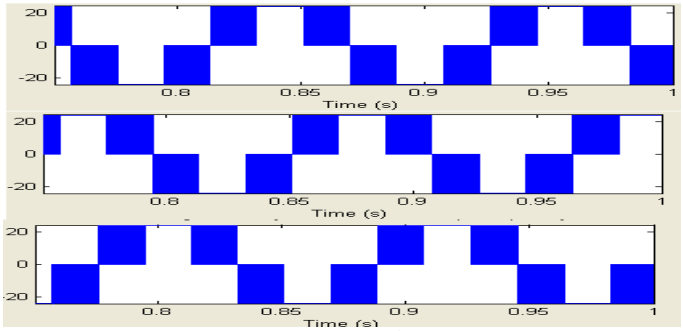

Fig8:- Phase voltage of inverter.

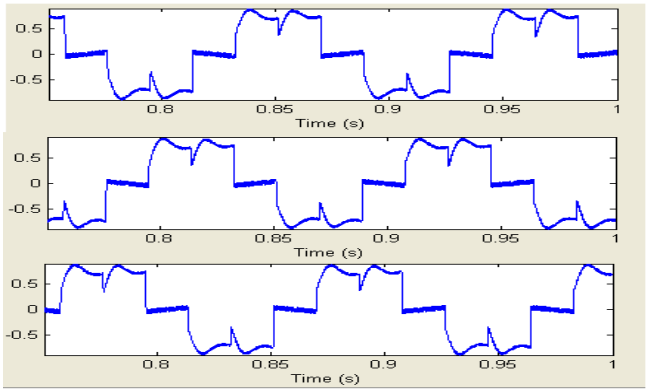

Fig9:- Output current of inverter.

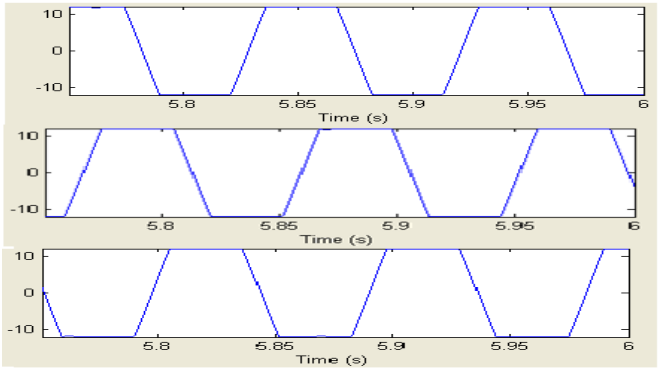

Fig:-10:-Back EMF waveform

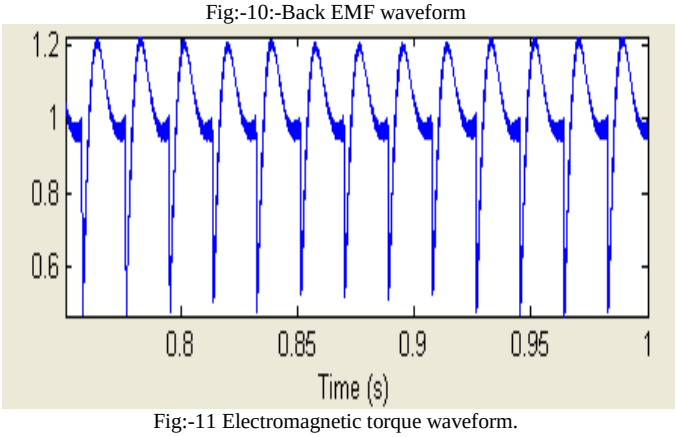

Fig:-11 Electromagnetic torque waveform.

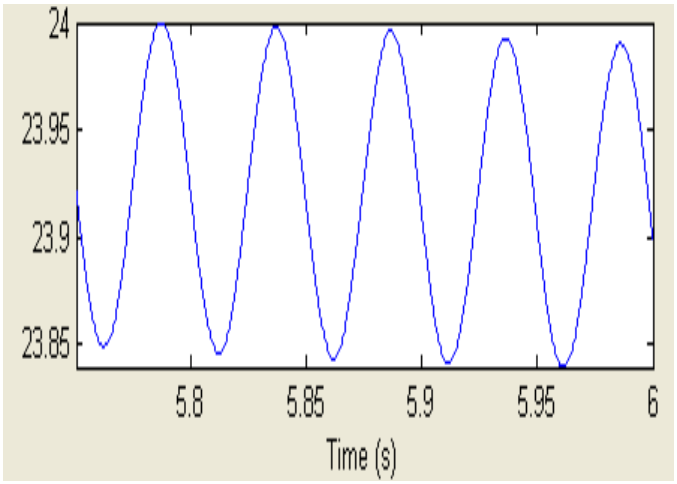

Fig : -12 Output of the buck converter

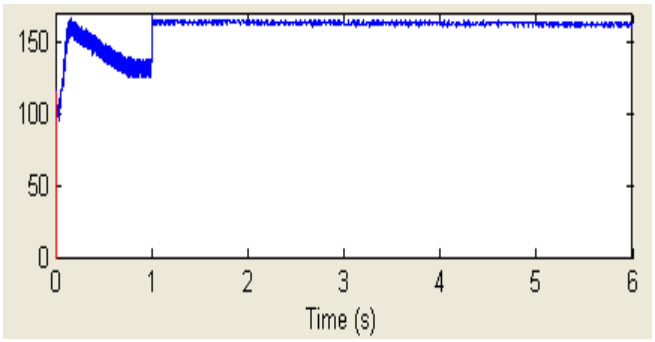

Fig:-5.13:-Rotor speed waveform.

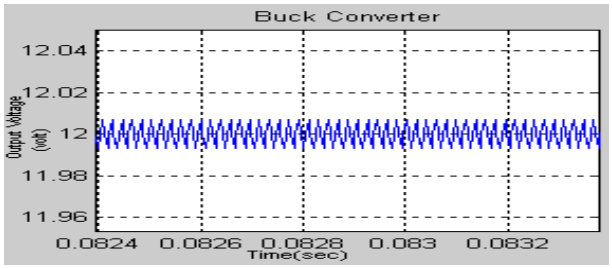

Fig 14 Buck Converter Output voltage

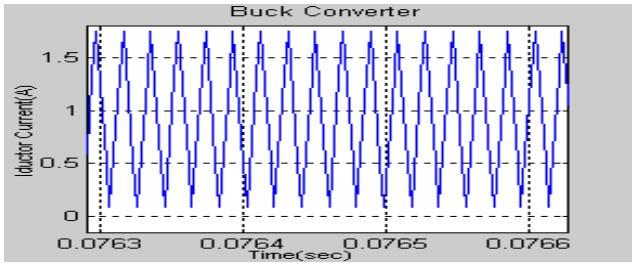

Fig. 15 Buck Converter Inductor Current

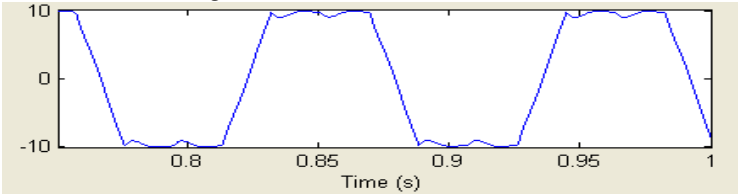

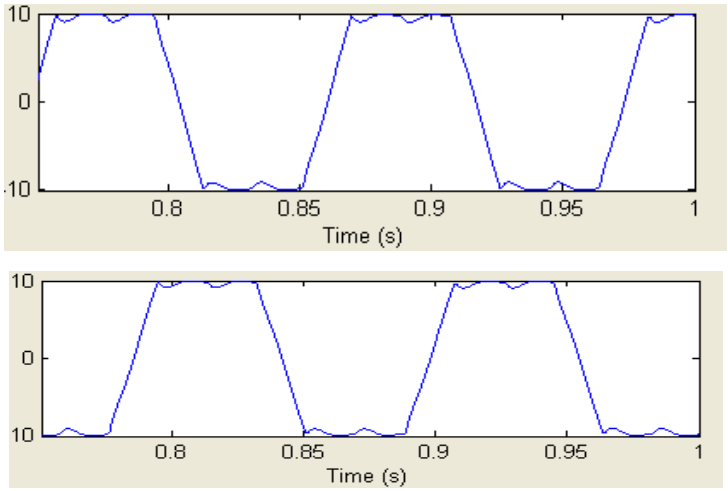

Fig. 16 Stator back emf a,b,c

Conclusion

The simulation and analysis of the electric vehicle DC-DC buck converter integrated with a Brushless DC (BLDC) motor using advanced MATLAB tools demonstrate a highly efficient and reliable power management system. The designed converter efficiently steps down the voltage, ensuring the motor operates within its optimal range. By leveraging the capabilities of BLDC motors, the system achieves enhanced energy efficiency, lower maintenance requirements, and superior performance characteristics suitable for electric vehicles.

The MATLAB simulations validate the system's performance under various load conditions, confirming the robustness and adaptability of the proposed design. This integration not only ensures smoother motor operation but also contributes to the overall system's sustainability by optimizing power usage. Future work could explore the integration of advanced control strategies, such as adaptive or predictive controllers, to further enhance the system's performance in real-world scenarios.

Reference

[1] Wei He, Nicholas Williard, Chaochao Chen, Michael Pecht “State of charge estimation for electric vehicle batteries using unscented kalman filtering” Microelectronics Reliability(2013), http://dx.doi.org/10.1016/j.microrel.2012.11.010

[2] Prashant Shrivastavaa, Tey Kok Soona,⁎, Mohd Yamani Idna Bin Idrisa, Saad Mekhilefb “Overview of model-based online state-of-charge estimation using Kalman filter family for lithium-ion batteries” Renewable and Sustainable Energy Reviews 113 (2019) 109233

[3] Xueqing Yuan, Lin Zhao, Bo Li, Naiming Liu “Battery Management System for Electric Vehicle and the Study of SOC Estimation” 2015 AASRI International Conference on Industrial Electronics and Applications (IEA 2015)

[4] Qiang Zhao, Cheng-Jun Shao, and Ying-Hua Han “
State of charge estimation for electric vehicle battery based on amended Ah metrology” Advances in Engineering Research (AER), volume 116 International Conference on Communication and Electronic Information Engineering (CEIE 2016)

[5] M. Surendar, P. Pradeepa “ Future Challenges in State of Charge Estimation for Lithium-Ion Batteries” International Journal of Engineering and Advanced Technology (IJEAT) ISSN: 2249-8958 (Online), Volume-10 Issue-1, October 2020.

[6] Omkar S Chitnis, Dr.M.S.Sheshgiri “A Review on Battery Management
System for Electric Vehicles” International Journal of Scientific & Engineering Research Volume 10, Issue 5, May-2019
ISSN 2229-5518

[7] A. Hariprasad1I. Priyanka2, R. Sandeep3, V. Ravi4, O. Shekar5 “Battery Management System in Electric Vehicles” International Journal of Engineering Research & Technology (IJERT) Vol. 9 Issue 05, May-2020

[8] Lora Khaula Amifia “Model Parameter Identification of State of Charge Based on ThreeBattery Modelling using Kalman Filter” Engineering Letters, 30:3, EL_30_3_24 revised July 6, 2022.

[9] Abbas Fotouhi, Karsten Propp and Daniel J. Auger “Electric Vehicle Battery Model Identification and State of Charge Estimation in Real World Driving Cycles” ceec 2015

[10] Ashwani Tapde, Asso. Prof. C S Sharma “Pmbldc Drive Closed Loop Controlled BuckConverter System” IJERA journal, Vol. 2, Issue 6, November- December 2012, pp.1101-1107.

[11] Ashwani Tapde, Rishi Maheshwari, Devendra Chandore “Low voltage start up closedloop control of buck converter fed unipolar PMBLDC motor” volume 3,issue 6, jul,2016

[12]H.J. Bergveld, Battery Management Systems Design by Modeling,2001, ISBN 9074445-51-9

[13] D. Bell, “A battery management system,” Master’s thesis, SchoolEng., Univ. Queensland, St. Lucia, Australia, 2000.

[14] Sandeep Dhameja, Electric Vehicle Battery Systems, 2002, ISBN0-7506-9916-7.

[15] K. Shimitzu, N. Shirai, and M. Nihei, “On-board batterymanagement system with SOC indicator,” in Proc. Int. ElectricVehicle Symp., vol. 2, 1996, pp. 99–104.

[16] Ng, K.S.; Moo, C.S.; Chen, Y.P.; Hsieh, Y.C. Enhanced coulombcounting method for estimating state-of-charge and state-of-healthof lithium-ion batteries. Appl. Energy 2009, 86, 1506–1511.
[17] Pattipati, B.; Pattipati, K.; Christopherson, J.P.; Namburu, S.M.;Prokhorov, D.V.; Qiao, L. Automotive Battery ManagementSystem. In Proceedings of IEEE AUTOTESTCON, Salt Lake City,UT, USA, 8–11 September 2008; pp. 581–586.